Experiments on the dynamics and stability of vortex pairs with axial core flow at high Reynolds numbers

Clément ROY & Thomas LEWEKE

Institut de Recherche sur les Phénomènes Hors Equilibre
CNRS / Universités Aix-Marseille, Marseille, France

Introduction – This presentation shows experimental results concerning the dynamics of two parallel (or nearly parallel) vortices at high Reynolds numbers (*Re*), which are characterised by the presence of an axial velocity defect. Co- and counter-rotating vortex pairs are studied in a wind tunnel and a water channel, with the goal of identifying and characterising a short-wave elliptic instability, which is expected to occur in this flow. In addition to the fundamental interest of this problem, a major application involving high-*Re* vortex pairs concerns the trailing wakes of transport aircraft and the associated danger for following aircraft, which imposes minimum separation distances in the vicinity of airports and limits air traffic capacity. Knowledge of the dynamics, instabilities and decay characteristics of the trailing vortex pairs is an important issue in this context.

Previous work on vortex pairs with axial flow include the wind tunnel studies of Devenport *et al.* [1, 2] and Jacquin *et al.* [3], who focused mainly on the turbulence characteristics of these flows. Experiments on the elliptic instability in vortex pairs *without* axial flow were carried out by Leweke and Williamson [6] and Meunier and Leweke [7]. This case has also been analysed in great detail theoretically and numerically (see, *e.g.*, [5]). Very little information is available, however, concerning the elliptic instability of vortices *with* axial flow. Some first theoretical results for the case of counter-rotating vortex pairs were presented recently by Lacaze [4]. The present study aims at providing more detailed information about this instability in realistic flow configurations.

Technical details – The present experiments were conducted in a closed-loop wind tunnel with a 0.8 m × 0.8 m square test section of length 4 m. The free stream turbulence intensity is less than 0.1% at the flow speeds used for this study. Two co-rotating vortices were generated by a symmetric NACA 0018 airfoil (0.4 m span, chord $c = 0.2$ m, rounded tip) mounted vertically at the test section ceiling, and equipped with a symmetric flap of chord 75 mm, which was fixed at 75% of the wing chord and extending from the root to 80% of the span. The wind tunnel was operated at its nominal maximum speed, resulting in a free stream velocity $U_o = 58.2$ m/s and a chord Reynolds number $Re_c = U_o c/\nu = 7.5 \times 10^5$, where ν is the kinematic viscosity of air at the constant temperature of 25°C. The angles of attack of the wing and the flap were fixed at 5° and 25°, respectively. Visualizations were achieved by injecting smoke near the flap and wing tips, and illuminating the flow with a sheet of light from a Nd-YAG pulsed laser. Measurements of the three-dimensional velocity field were carried out at different positions downstream of the wing by hot wire anemometry, using a three-wire probe by Dantec (model 55P91), in combination with calibration and post-processing algorithms based on the work of Wittmer *et al.* [8].

In parallel, dye visualisations of counter- and co-rotating vortex pairs were obtained in a free-surface water channel, with a test section of length 150 cm, width 37 cm, and depth 50 cm. Here, the two vortices were generated by two independent airfoils (NACA 0012, chord 10 mm, rounded tips), placed vertically on the bottom wall and a support outside the free surface, with the two tips facing each other. The free stream velocity was 90 cm/s, leading to a chord Reynolds number $Re_c = 9.0 \times 10^2$, an order of magnitude lower than the wind tunnel flow. Visualisation of the vortex core structure was achieved by injection of fluorescent dye near the wing tips, and illumination by the light of a continuous Argon ion laser.

Results – Figure 1 shows a series of instantaneous visualisations of the co-rotating vortex pair behind the flapped wing in the wind tunnel at $Re_c = 7.5 \times 10^5$. The mutually induced rotation around each other, as the vortices move downstream, is clearly seen. From the separation distance of the vortices and the orientation angle of the pair, as function of downstream distance x (measured from the trailing edge of the wing), one can determine the total circulation of the flow. Together with the hot wire measurements (see below), one finds that the vortices have an almost equal circulation, with the vortex Reynolds number $Re_\Gamma = \Gamma/\nu$ being close to $Re_\Gamma = 1.2 \times 10^5$. At each downstream position, a large number of instantaneous images were taken, in order to characterise the apparently random transverse motion of the vortices, often referred to as meandering. The amplitude of this motion was found to increase quite drastically between $x/c = 8.5$ and $x/c = 11.2$. Measurements at $x/c = 13.8$ (not represented in figure 1) do not show two well distinguished vortices any more, *i.e.*, the merging of the two into a single final vortex has set in at this point.

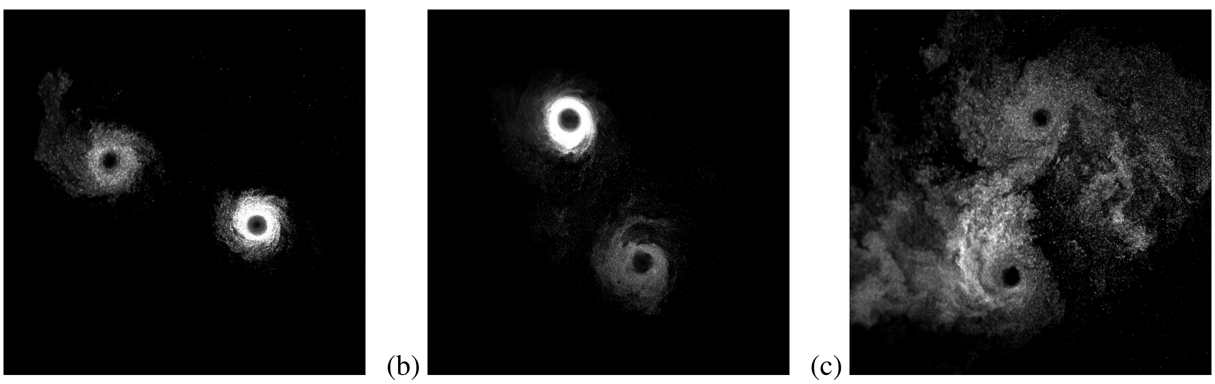

(a) (b) (c)

Figure 1: Smoke visualisation of a corotating vortex pair behind a flapped wing extending vertically (tip at bottom). The downstream positions are (a) $x/c = 2.0$, (b) $x/c = 8.5$, and (c) $x/c = 11.2$. The wing tip vortex is marked by the brighter smoke pattern.

For a precise comparison with theoretical predictions and planned numerical simulations, the velocity profiles of the vortices have to be known accurately. Figure 2 shows the overall distributions of the mean longitudinal (axial) velocity U_x and vorticity ω_x in the cross-sectional plane at $x/c = 8.5$. The velocity defect induced by the presence of the wing can been seen at the upper right of figure 2(a). At this station, the pair has undergone more than half a rotation. From measurements as in figure 2, with a high spatial resolution near the vortex centres, one can obtain the mean velocity profiles of each vortex. The result for $x/c = 8.5$ is shown in figure 3. The core size a, *i.e.*, the radius of maximum azimuthal velocity U_θ, is found to be only about 3% of the wing chord for the tip vortex, and around 5% for the flap vortex. The axial velocity defect seems to have a slightly larger radial scale than the swirl velocity. The velocity defect is significantly higher in the flap tip vortex.

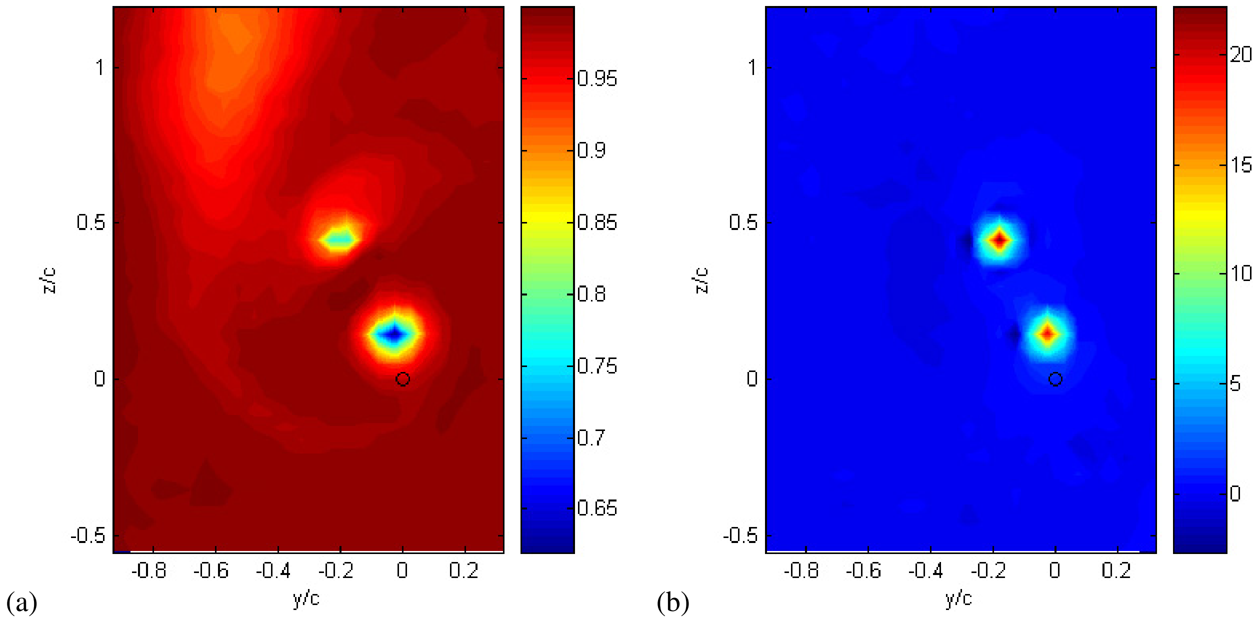

Figure 2: Mean flow field behind the flapped wing at $x/c = 8.5$, corresponding to the visualisation in figure 1(b). (a) Distribution of axial velocity U_x/U_o; (b) vorticity $\omega_x c/U_o$.

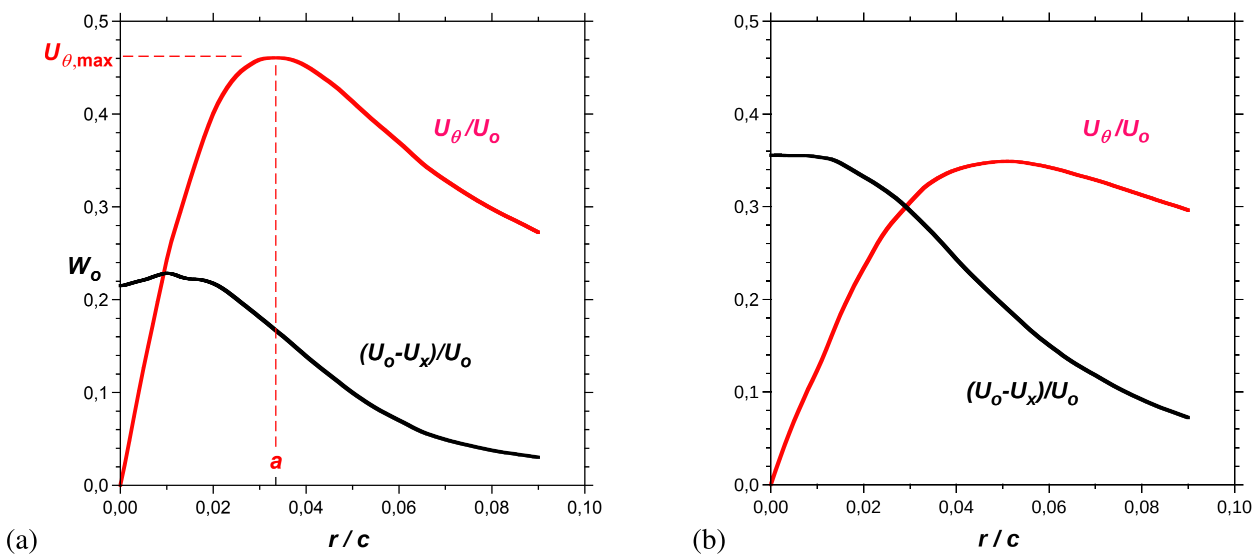

Figure 3: Azimuthally averaged velocity profiles of the vortices at $x/c = 8.5$.
(a) Wing tip vortex, (b) flap tip vortex.

	wing tip vortex			**flap tip vortex**		
x/c	a/c	W_o/U_o	$U_{\theta,\max}/U_o$	a/c	W_o/U_o	$U_{\theta,\max}/U_o$
8.5	0.033	0.22	0.46	0.051	0.36	0.35
11.2	0.071	0.15	0.20	0.085	0.24	0.22
13.8	-	0.11	-	-	0.12	-

Table 1: Vortex parameters.

The main vortex parameters deduced from these measurements are summarised in table 1. As expected, the core size increases, and the maximum velocity defect and swirl velocity decrease with downstream distance. However, these quantities are so far calculated from time-averaged measurements. A precise analysis, taking into account the information concerning vortex meandering obtained from the visualisations is underway. At $x/c = 13.8$, the merging has well advanced, and only two slight defects of axial velocity can be detected. The meandering is quite vigourous for $x/c > 10$. It is not clear if this is linked to the development of an instability, possibly of the elliptic type. Although the velocity fluctuations and turbulence levels are high near the vortex centres, spectral analysis of the time series have so far not revealed a characteristic frequency corresponding to a possible instability wavelength. Two-point correlation measurements are planned, as well as a forcing of particular wavelengths in the flow.

Flow visualisation of a co-rotating vortex pair in the water channel has revealed a very similar behaviour: the vortices merge after about one revolution around each other and perturbations grow on the vortices, involving a displacement of the core, which could be associated with meandering; they are clearly visible just before merging. Preliminary visualisations of co-rotating vortex pairs seem to reveal a different kind of short-wave perturbation, involving internal core deformations. This is a more promising sign of elliptic instability.

More details on the water tunnel results and on the observations discussed above, including some information on the experimental difficulties one faces when trying to obtain reliable data on high-Reynolds number slender vortices, will be presented at the conference.

This work is supported by the European Commission under Contract No. AST4-CT-2005-012338 (FAR-Wake).

References

[1] W. J. Devenport, J. S. Zsoldos, and C. M. Vogel 1997. *The structure and development of a counter-rotating wing-tip vortex pair*, J. Fluid Mech. **332**, 71–104.

[2] W. J. Devenport, C. M. Vogel, and J. S. Zsoldos 1999. *Flow structure produced by the interaction and merger of a pair of co-rotating wing-tip vortices*, J. Fluid Mech. **394**, 357–377.

[3] L. Jacquin, D. Fabre, P. Geffroy, and E. Coustols 2001. *The properties of a transport aircraft wake in the extended near-wake field: an experimental study*, AIAA Paper 2001-1038.

[4] L. Lacaze 2005. *L'instabilité elliptique : exemples en aéronautique et en géophysique*, Ph.D. thesis, Université de Provence, Marseille, France).

[5] S. Le Dizès and F. Laporte 2002. *Theoretical predictions for the elliptical instability in a two-vortex flow*, J. Fluid Mech. **471**, 169–201.

[6] T. Leweke and C. H. K. Williamson 1998. *Cooperative elliptic instability of a vortex pair*, J. Fluid Mech. **360**, 85–119.

[7] P. Meunier and T. Leweke 2005. *Elliptic instability of a co-rotating vortex pair*, J. Fluid Mech. **533**, 125–159.

[8] K. S. Wittmer, W. J. Devenport, and J. S. Zsoldos 1998. *A four-sensor hot-wire probe system for three-component velocity measurement*, Exp. Fluids **24**, 416–423.